International Journal of Botany Studies
ISSN: 2455-541X
Impact Factor: RJIF 5.12
www.botanyjournals.com
Volume 3; Issue 1; January 2018; Page No. 17-20

Comparison of X-ray broadening studies of MEA and *G. superba* capped CeO_2 nanoparticles

Biju Joy
Department of Chemistry, St. Xavier's College, Thumba, Trivandrum, Kerala, India

Abstract
The Monoethanolamine (MEA) capped cerium oxide Nanoparticles (CeO_2 NPs: B1) and *Gloriosa superba* (*G. superba*) capped CeO_2 NPs (B2) were synthesized through co-precipitation and Green method. X-ray diffraction (XRD) studies revealed that**,** synthesized both CeO_2 exhibits were retained the cubic structure. The crystallite sizes and lattice strain to the peak broadening in MEA and *G. superba* capped CeO_2 NPs were studied using Williamson-Hall (W-H) analysis. In FESEM image analysis, the MEA and *G. superba* CeO_2 NPs morphology were formed spherical shape. Elemental compositions of Ce and O percentage were identify by EDAX spectra.

Keywords: monoethanolamine, green method, CeO_2 NPs, and williamson-hall analysis

1. Introduction
CeO_2 NPs are used for a wide range of applications, such as an electrolyte in solid oxide fuel cells, oxygen gas sensors, a support in automotive catalysts, a polishing agent in chemical mechanical polishing, and an ultraviolet shielding material (Esposito and Enrico., 2008, Armini *et al*., 2008) [1, 2]. Generally, syntheses of nanoparticles have been achieved by several methods incorporated with physical and chemical way, such as hydrothermal, flame spray pyrolysis, sonochemical, microwave, sol-gel, and co-precipitation methods (Zhang *et al*., 2002., Hu *et al*., 2007, Wang *et al*., 2002, Liao *et al*., 2001, Czerwinski *et al*., 1997, and Yao and Xie., 2007) [3-8]. Though, these approaches are the most relevant methods. But also these techniques are involving complex procedures, time taken, expensive and hazardous chemicals. As a result of these confines, the green chemistry attitudes are remarkably considered to be the most worth protocol in the phyto-synthesis of metal oxide NPs owing to their plenty of rewards such as cost-effectiveness, large-scale commercial production, environment-friendly and pharmaceutical applications (Arumugam *et al*., (2015)) [9].
A perfect crystal would extant infinitely in all directions; therefore, no crystals are perfect due to their finite size. This deviation from perfect crystallinity leads to broadening of the diffraction. The two main properties extracted from the peak width analysis are the crystallite size and the lattice strain. The crystallite size is a measure of the size of coherently diffracting domains. The crystallite size of the particles is generally not the same as the particle size due to the formation of polycrystalline aggregates (Ramakanth., 2007) [10]. To determine the particle size using X-ray powder diffraction (XRPD) measurements, the Scherer's formula is the simplest method to the calculate crystallite size, and is applicable only when there is no strain in the materials. The other analytical method such as Williamson-Hall (W-H) is generally used to determine the strain and the crystallite size of nanomaterials.
In the present work, MEA capped CeO_2 and *G. superba* capped CeO_2 NPs synthesized by co-precipitation method and green method. From this result, a comparative studies of the average particle size of MEA capped CeO_2 and *G. superba* capped CeO_2 NPs obtained from FESEM measurements and from powder XRD procedures are being reported. The strain due to lattice deformation association with CeO_2 NPs capping with MEA and *G. superba* plant extract was calculated by Williamson-Hall (W-H) plots.

2. Materials and Method
The following high purity chemicals such as Cerium nitrate, Monoethanolamine (MEA), and Sodium hydroxide were used as precursors without further purification.
The MEA added CeO_2 NPs synthesis following, Cerium Nitrate 0.1 M a with capping agent added MEA 0.05M were dissolved double distilled water separate 100 ml beaker, then form a homogenous mixture. 0.8 M of NaOH was separately dissolved in 100 ml of double distilled water. Then, NaOH solution was added drop wise to the homogenous mixture of Cerium nitrate solution, the pH 12.30 obtained and which yields violet precipitate. The solution with the violet precipitate was stirred at room temperature for 6 h. This solution was refluxed at room temperature for 24 h. Then, a clear solution was obtained, which found to be stable at ambient condition.
The 10 g of *G. superba* finely cut green leaves were added to 100 mL of double distilled water and boiled at 50-60 °C for 15 min. The obtained extraction was filtered using Whatmann No. 1. Thereafter, 0.1M of Ce $(NO_3)_3.6H_2O$ salt was added to 100 mL of *G. superba* leaf extract. This solution was stirred constantly at 80 °C temperature for 6h. A brown precipitate formed and then it was becoming a yellowish brown in color on continuous stirring. A schematic diagram of *G. superba* capped CeO_2 NPs is shown in Fig. 1.
Thereafter, the solution was washed several times with double distilled water and ethanol. The precipitate was dried at 120 ˚C. Finally, MEA capped CeO_2 and *G. superba* capped CeO_2

NP samples were annealed at 700 ºC for 5 h.

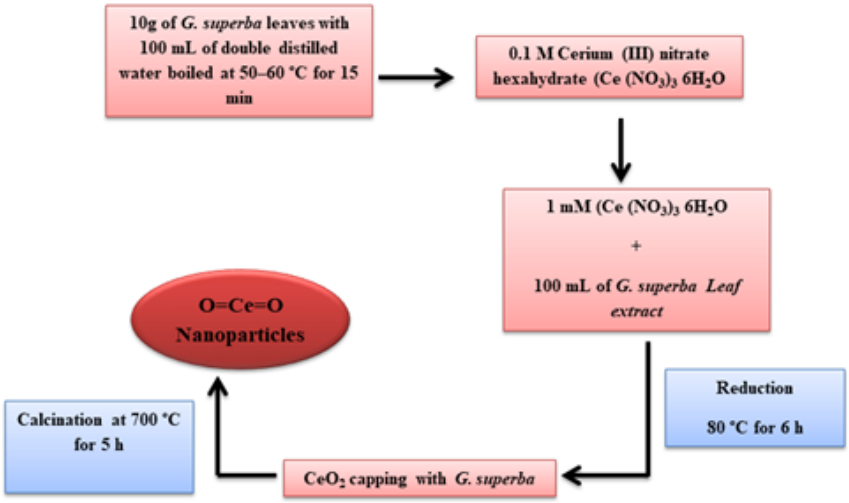

Fig 1: A schematic diagram of *G. superba* capped CeO_2 NPs.

2.1 Characterization Techniques

The MEA capped CeO_2 and *G. superba* capped CeO_2 NPs were characterized by X-ray diffractometer (model: X'PERT PRO PANalytical). The diffraction patterns were recorded in the range of 30º-80º for the MEA capped CeO_2 and *G. superba* capped CeO_2 NP samples where the monochromatic wavelength of 1.54 Å was used. The samples were analyzed by Field Emission Scanning Electron Microscopy (Carl Zeiss Ultra 55 FESEM) with EDAX (model: Inca).

3. Results and discussion

3.1 X-ray diffraction studies

Figure 2 shows the XRD patterns of as-synthesized MEA and *G. superba* capped CeO_2 NPs. The XRD peaks are located at angles (2θ) of (28.58, 33.13, 47.53, 56.38, 59.09, 69.46 and 76.73) and (28.59, 33.12, 47.54, 56.40, 59.1, 69.48, and 76.7) corresponding to (111), (200), (220), (311), (222), (400), (331) and (420) planes of the both MEA and *G. superba* capped CeO_2 NPs. The standard diffraction peak shows the face-center cubic phase of CeO_2 NPs (JCPDS data card no: 34-0394). To examine the effect of *G. superba* capped CeO_2 NPs on structure, an enlarged version of the XRD pattern between 27.5˚ and 29.5˚ is shown in Fig. 3. It is worthy to mention that there is slight lower angle shift as compared to MEA capped CeO_2 NPs. The micro-strain analysis is a performed for the samples from the XRD diffraction. The breadth of the Bragg peak is a combination of both instrument and sample-dependent effects. To decouple these contributions, it's necessary to collect a diffraction pattern from the line broadening of a standard material such as silicon to determine the instrumental broadening. The instrument-corrected broadening β_{hkl} (Ramakanth., 2007) [10] can be represented by:

$$\beta_{hkl} = [\ \beta_{hkl}^2 measured - \beta_{hkl}^2 instrumental\ ]^{1/2}$$

The crystallite size of MEA and *G. superba* capped CeO_2 NPs are determined by the X-ray line broadening method using the Scherrer's equation,

$$D = k\lambda/\beta(D\cos\theta)$$

Where D is the size in nanometers, λ is the wavelength of the radiation (1.5406Å for CuKα), k is a constant (0.94), β_D is the peak width at half-maximum intensity and θ is the peak position. The MEA and *G. superba* capped CeO_2 NPs average crystallite sizes are observed at 21.56 nm and 18.71 nm respectively. The crystallite size of *G. superba* capped CeO_2 NPs decreased as compared to that of MEA capped CeO_2 NPs. The reduction in the crystallite size is mainly due to the many organic components involved in the formation of nanoparticles, which is decrease the nucleation and subsequent growth rate of the CeO_2 NPs.

The strain-induced broadening βε is given by the Wilson formula $\beta\varepsilon = 4\varepsilon\tan\theta$, where ε is the root mean square value of the micro-strain. Assuming that the particles size and strain contributing to the line broadening and independent of each other and both have a Cauchy like profile, the observed line width is simply the sum of these two, i.e., $\beta_{hkl} = (k\lambda / D\cos\theta) + 4\varepsilon\tan\theta$, which becomes as

$$\beta_{hkl}\cos\theta = (k\lambda/D) + 4\varepsilon\sin\theta$$

When plotting the Williamson-Hall equation between 4sinθ Vs β cosθ the slope of the line is the strain ε. Figures 4 (a-b) show the plots of Williamson-Hall equation for MEA and *G. superba* capped CeO_2 NPs samples. The calculated strain values are 0.00608 and 0.00787 for MEA and *G. superba* capped CeO_2 NPs respectively. The strain of *G. superba* capped CeO_2 NPs increased as compared to that of the MEA capped CeO_2 NPs, which is due to the relaxation of the strain in the respective unit cells. These effects change the size and shape of the particles.

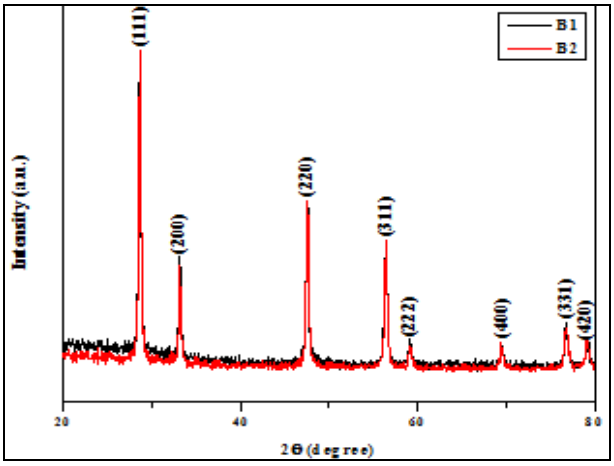

Fig 2: X-ray diffraction pattern of MEA and *G. superba* capped CeO_2 NPs.

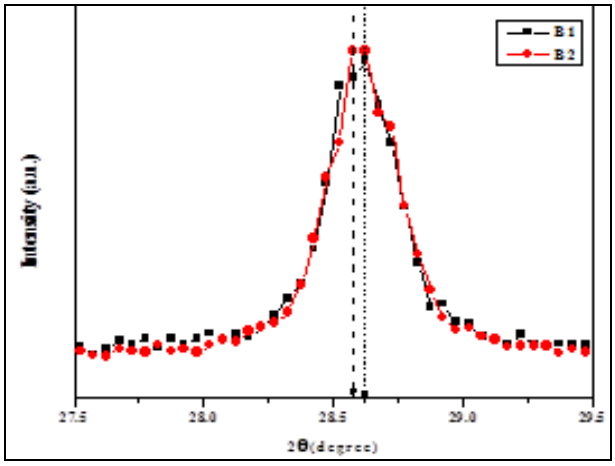

Fig 3: an enlarged version of the XRD pattern between 31° to 32.5°.

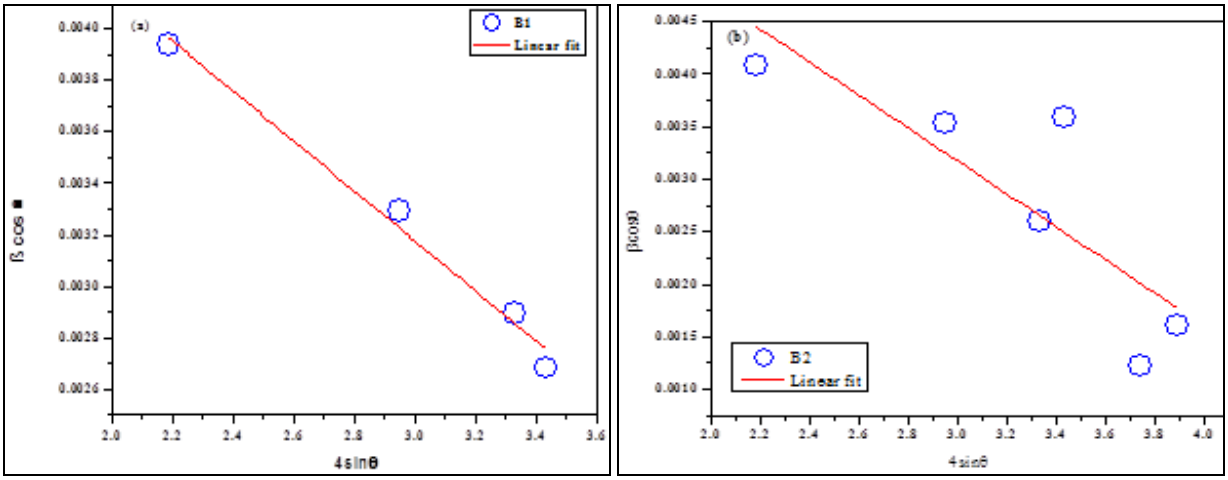

Fig 4: The Williamson-Hall of (a) MEA capped CeO_2 NPs and (b) *G. superba* capped CeO_2 NPs.

3.2 Morphology and elemental composition analysis

FESEM images show the morphological analysis of synthesized MEA and *G. superba* capped CeO_2 NPs are shown in Fig. 5 (a-b). The synthesized MEA and *G. superba* capped CeO_2 NPs are formed cubic structure and average particle size are observed at 35 and 27 nm. This size reduction may be presence of various organic components involved in the NPs formation. Metal element composition of CeO_2 NPs as shown in Fig. 3(c-d). From EDAX results, the Ce and O atomic percentage are observed at (31.13 % & 68.87%) and (73.62 % & 26.38%) for MEA capped CeO_2 and *G. superba* capped CeO_2 NPs respectively. The *G. superba* capped CeO_2 NPs oxygen percentage increase with decrease the cerium percentage as compared to that of MEA capped CeO_2 NPs, which may be NPs formed using *G. superba* plant extract.

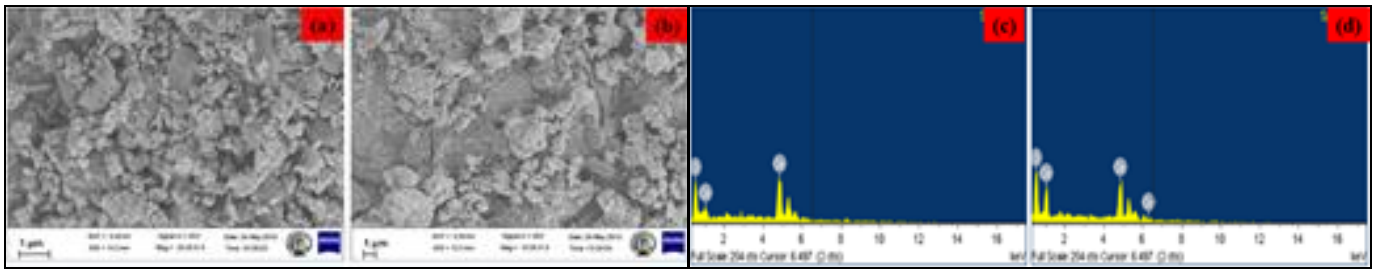

Fig 5: (a-b) FESEM image of MEA and *G. superba* capped CeO_2 NPs and (c-d) EDAX spectra of MEA and *G. superba* capped CeO_2 NPs.

4. Conclusions

In summary, MEA and *G. superba* capped CeO_2 NPs were synthesized through co-precipitation and Green method. The synthesized CeO_2 NPs were exhibited face-centered cubic structure. Crystalline size of *G. superba* capped CeO_2 NPs possess decreased as compared to MEA capped CeO_2 NPs, The reduction in the crystallite size was mainly due to the many organic components involved in the NPs formations.

The line broadening synthesized CeO_2 NPs, *G. superba* plant capping effects, decreased crystallite size and increases lattice strains. The broadening was analyzed by the Scherrer formula, modified forms of W-H analysis. From FESEM images, the MEA and *G. superba* capped CeO_2 NPs were formed cubic structure and average particle size were calculated at 35 and 27 nm. From the EDAX spectra, the elemental composition was identified.

5. References

1. Esposito V, Traversa E. Design of electroceramics for solid oxides fuel cell applications: playing with ceria. Journal of the American Ceramic Society. 2008; 91(4):1037-51.
2. Armini S, De Messemaeker J, Whelan CM, Moinpour M, Maex K. Composite polymer core–ceria shell abrasive particles during oxide cmp: A defectivity study. Journal of the Electrochemical Society. 2008; 155(9):H653-60.
3. Zhang F, Chan SW, Spanier JE, Apak E, Jin Q, Robinson RD *et al*. Cerium oxide nanoparticles: size-selective formation and structure analysis. Applied physics letters. 2002; 80(1):127-9.
4. Hu JD, Li YX, Zhou XZ, Cai MX. Preparation and characterization of ceria nanoparticles using crystalline hydrate cerium propionate as precursor. Materials Letters. 2007; 61(28):4989-92.
5. Wang H, Zhu JJ, Zhu JM, Liao XH, Xu S, Ding T *et al*. Preparation of nanocrystalline ceria particles by sonochemical and microwave assisted heating methods. Physical Chemistry Chemical Physics. 2002; 4(15):3794-9.
6. Liao XH, Zhu JM, Zhu JJ, Xu JZ, Chen HY. Preparation of monodispersed nanocrystalline CeO_2 powders by microwave irradiation. Chemical Communications. 2001 (10):937-8.
7. Czerwinski F, Szpunar JA. The nanocrystalline ceria sol-gel coatings for high temperature applications. Journal of Sol-Gel Science and Technology. 1997; 9(1):103-14.
8. Yao SY, Xie ZH. Deagglomeration treatment in the synthesis of doped-ceria nanoparticles via coprecipitation route. Journal of materials processing technology. 2007; 186(1):54-9.
9. Arumugam A, Karthikeyan C, Hameed ASH, Gopinath K, Gowri S, Karthika V *et al*. Synthesis of cerium oxide nanoparticles using Gloriosa superba L. leaf extract and their structural, optical and antibacterial properties. Materials Science and Engineering, 2015; 49:408-415.
10. Ramakanth K. Basics of X-ray Diffraction and its Application. IK, New Delhi. 2007.